Experimental Investigation of the Boundary Layer on a Rotating Cylinder

J. B. Morton,* Ira D. Jacobson,† and Seldon Saunders‡
University of Virginia, Charlottesville, Va.

This paper documents the experimental analyses done in determining the stability, transition, and growth of boundary layers on a spinning cylinder at angle of attack. It has been shown that spin alters the boundary-layer growth as well as skewing and moving forward the transition line. These effects can have a significant influence on the thickness distribution of the boundary layer.

Nomenclature

f	= audio frequency
F	= signal frequency
r	= body radius, 5.72 cm
$R=\frac{V_\infty \delta}{\upsilon}$	= Reynolds number based on boundary-layer thickness
$Re=\frac{V_\infty x}{\upsilon}$	= Reynolds number based on length
u'	= turbulent velocity fluctuation
$U(y)$	= velocity component along axis of cylinder
V_∞	= freestream velocity
$W(y)$	= crossflow velocity
x, y, z	= body coordinates (c.f., Fig. 1)
α	= angle of attack
δ	= boundary-layer thickness
δ_0	= boundary-layer thickness at which $U(y)=0.9\ V_\infty$ (no spin)
δ_s	= boundary-layer thickness at which $U(y)=0.9\ V_\infty$ (with spin)
η	= boundary-layer coordinate y/x $(V_\infty x/\upsilon)$
υ	= kinematic viscosity
θ	= aximuthal position around cylinder (z/a)
ω	= spin rate

Introduction

THE purpose of these studies is to provide data for understanding the relationship between the boundary-layer behavior on spinning bodies at angle of attack and the Magnus effect. Some previous work has been done experimentally by Thorman[1] and Fehrman,[2] who investigated the boundary-layer growth and transition on a spinning ogive; by Furuya, Nakamura, and Kawachi,[3] who measured the momentum thickness on a spinning body of revolution which was unyawed; and by Jacobson,[4] who measured transition lines on a yawed spinning semi-infinite cylinder. Sturek[5,6] measured boundary layers on a spinning cone and a spinning tangent-ogive-cylinder. Predictions of the effect of spin on the thickness of the laminar boundary layer on a yawed cylinder were made by Martin,[7] and these were used to calculate the Magnus effect. For a complete review, see Jacobson.[9]

Experimental Facility

The wind-tunnel model used to investigate the stability, growth rates, and other features of the boundary layer on a rotating cylinder is shown schematically in Fig. 1. The model was installed in a 100 cm × 150 cm subsonic tunnel. A hot-wire probe is remotely positioned in the boundary layer by a traversing mechanism with three degrees of freedom: x, the longitudinal distance along the cylinder; y, the radial distance from the cylinder; and z, the distance along the circumference of the cylinder. The traversing mechanism can also be adjusted so that the probe may be positioned at any angle about the axis of the cylinder. Tests were conducted at a freestream velocity of 34 fps.

As shown in Fig. 1, there are several unique features incorporated in the design of the model. First, an annular suction slot is used at the nose of the model to remove all of the boundary layer which develops along the nose. In this way, the effect of the particular design of the nose upon the flow on the cylindrical test section is eliminated.

The second feature concerns the injection of a velocity perturbation into the boundary layer through the use of a tuned acoustic driver which sets up standing waves within the interior of the cylinder. These waves interact with the flow through the annular suction slot to produce the desired signal. Hot-wire measurements show that this signal is confined almost entirely to the boundary layer. The growth and decay of this signal is tracked along the body and the coordinate of the maximum and minimum points of the perturbation serve to determine the location of the neutral stability curve.

A third aspect of the model design is the use of an annular disk suction slot located to the rear of the rotating test section. By adjusting the suction flow rate through this slot, the longitudinal pressure gradient along the cylinder is removed without resorting to cumbersome tunnel wall adjustments.

Since reported measurements of the neutral stability curve for a flat plate show considerable scatter, a two-channel hot-wire measuring system was used to improve the consistency of the results. A fixed hot-wire is positioned in the boundary layer near the middle of the cylinder and is used to monitor the signal. Any change in the effective Reynolds number or in the injected signal strength immediately shows up as a change

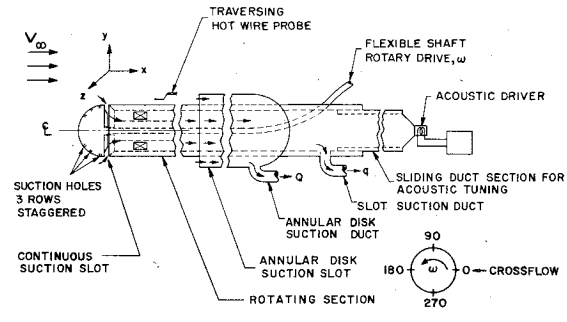

Fig. 1 Model schematic.

Received Feb. 2, 1976; revision received June 7, 1976. Work supported by the Ballistic Research Laboratories, Aberdeen Proving Ground, Contract No. DAAD05-72-C-0131.

Index categories: Boundary-Layer Stability and Transition.

*Associate Professor, Dept. of Engineering Science and Systems. Member AIAA.

†Associate Professor, Dept. of Engineering Science and Systems. Member AIAA.

‡Graduate Research Assistant, Dept. of Engineering Science and Systems.

in the fixed wire signal, and thus false readings are avoided. The second hot-wire is located on the opposite side of the model. A flexible traversing mechanism allows this wire to be used to trace the growth of the boundary layer and the velocity fluctuation.

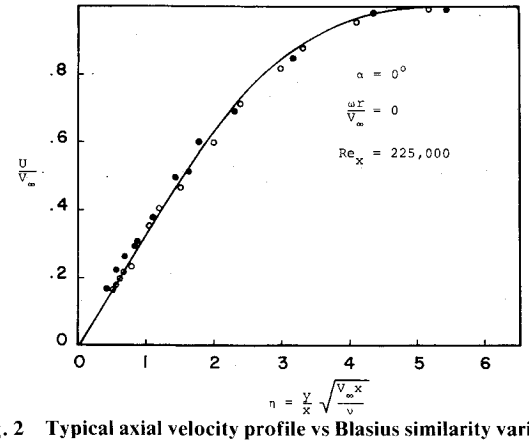

Fig. 2 Typical axial velocity profile vs Blasius similarity variable.

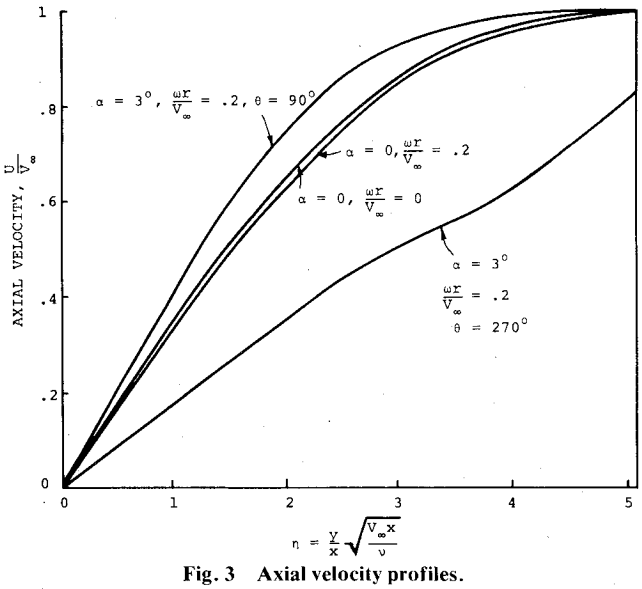

Fig. 3 Axial velocity profiles.

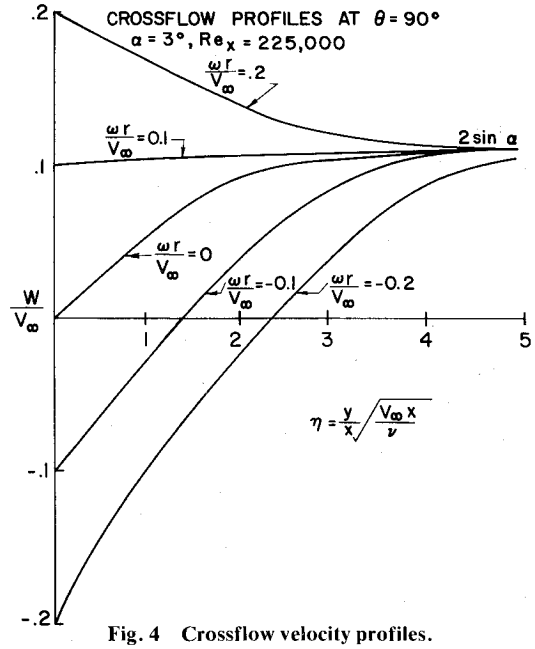

Fig. 4 Crossflow velocity profiles.

The output of each hot-wire is linearized and fed through a narrow band filter tuned to the acoustic driver frequency. The amplitudes of the filter output then represent the magnitude of the perturbation u'. This signal is squared, averaged, and read by a digital voltmeter. The dc level of the output of the linearizer is also monitored using a digital voltmeter so that mean velocity profiles may be obtained. The velocity profile is

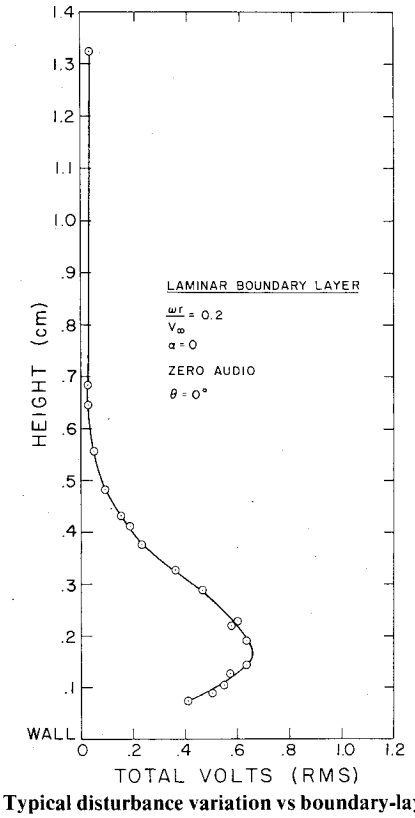

Fig. 5 Typical disturbance variation vs boundary-layer height.

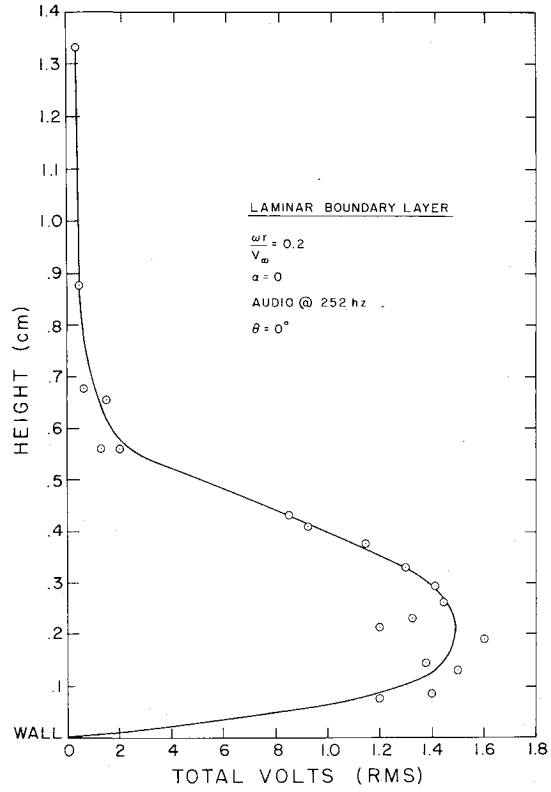

Fig. 6 Typical disturbance variation vs boundary-layer height.

used to determine a virtual origin for the boundary layer which is needed to calculate the critical Reynolds number. The rest of the parameters important for the experiment are measured in straightforward fashion.

Experimental Data

Typical velocity profiles are shown in Figs. 2 through 4. Figure 2 for the zero angle-of-attack, zero spin case indicates the scatter in the data about the theoretically expected Biasius profile. Figures 3 and 4 show typical profiles of both the axial and crossflow velocity profiles vs angle of attack, spin rate, and azimuthal position. Measurements of the variation of the boundary-layer disturbances were also made. For a fixed angle of attack, spin rate, and azimuthal position, the laminar boundary-layer disturbance varies with height. Typical variations are shown in Figs. 5 and 6. As can be seen, the major effect of the audio signal is to amplify the peak disturbance without altering the general shape of the curve.

The effectiveness of the signal injection and measurement system may be judged from photos shown in Fig. 7. These photos were made using an oscilloscope simultaneously displaying the traversing and reference linearized hot-wire outputs. In the first photograph, the traversing hot-wire is located 19 cm to the rear of the suction slot and at a value of y where the u' signal is found to a maximum. The reference wire is always located a 34 cm from the suction slot at the y value which gives the largest signal. In the second photograph, the traversing wire has been placed 34 cm to the rear of the last slot. Again, the wire is traversed radially along y to find the maximum value of u'. Clearly, the maximum of the u' signal has increased between these two stations. In the last photograph, the traversing wire has been positioned at $x=49$ cm and at a y value where u' is again a maximum. At this x the u' signal has decayed, indicating that there must be a maximum of the signal between 19 and 48 cm. This maximum is found to be quite close to the location where $x=34$, and thus the Reynolds number corresponding to this location lies on the upper branch of the neutral stability curve at a frequency corresponding to the injected signal frequency. Tracking this disturbance yields the Reynolds number associated with decay and with growth (Fig. 8) defining the neutral stability curve.

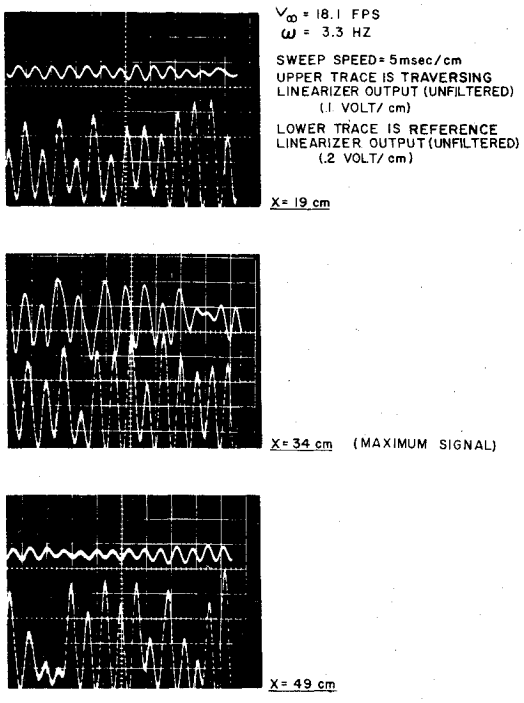

Fig. 7 Hot-wire signal.

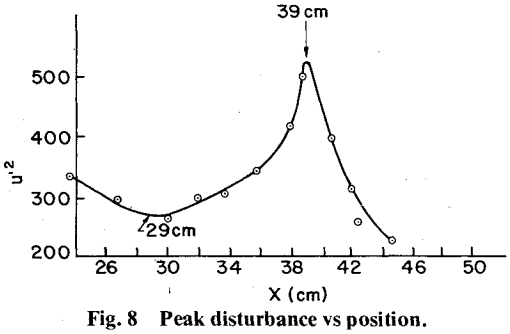

Fig. 8 Peak disturbance vs position.

Results of these measurements are shown in Fig. 9 where the measured points of the neutral stability curve for the case of zero angle of attack and zero spin rate are plotted as solid dots for various values of signal frequency F and Reynolds number R where

$$F=\frac{2\pi f\nu}{V_\infty^2}$$

$$R=\frac{V\delta_\infty}{\nu}$$

The solid line represents the theoretical results of Barry and Ross[8] for the corresponding flat-plate boundary layer.

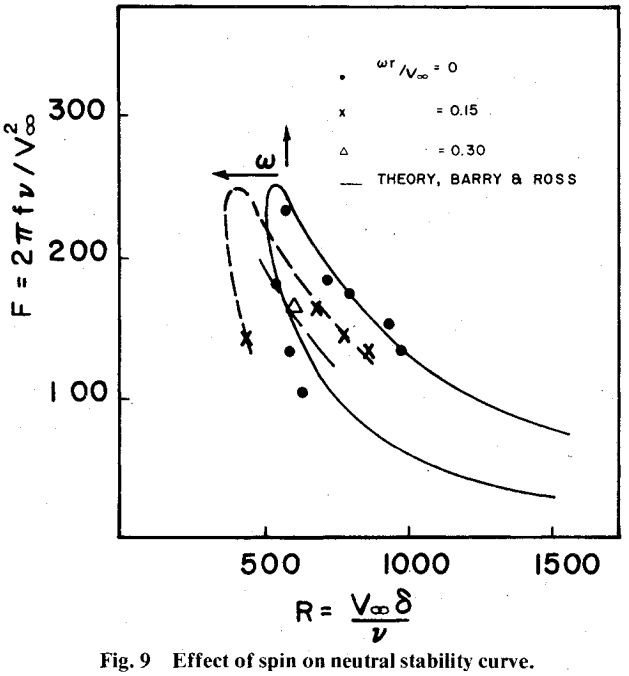

Fig. 9 Effect of spin on neutral stability curve.

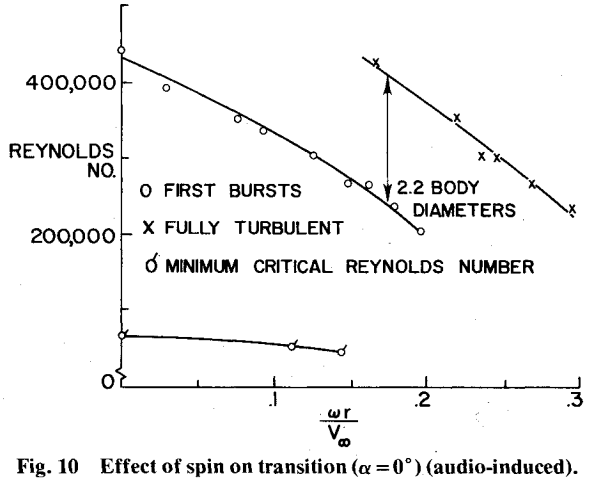

Fig. 10 Effect of spin on transition ($\alpha=0°$) (audio-induced).

The crosses in Fig. 9 represent data taken at zero angle of attack but with the cylinder spinning. The dashed line is drawn in to indicate how the entire neutral stability curve is shifted to the left by spin. A further increase in spin shifts the curve even further to the left, as indicated by the triangular data point in Fig. 9.

The beginning of transition (first bursts) and fully turbulent flow for the zero angle of attack case are shown in Fig. 10. At each point the hot-wire was adjusted to the value of y which gave the earliest indication. The spin rates for first bursts and fully turbulent flow were determined by slowly adjusting the spin rate and observing the signal on an oscilloscope. Here it is seen that the effect of spin on reducing the Reynolds number for first bursts and full transition is greatly amplified over the trend indicated for the minimum critical Reynolds number. As spin is increased, the transition line moves toward the leading edge as well as being skewed azimuthally; both effects can contribute to an increasing turbulence level at some stations.

At angle of attack the effect of spin on transition was examined using a microphone placed on the output of a pitot tube. The signal produced was displayed on an oscilloscope. The pitot tube was traversed along the cylinder and changes in the signal indicated transition location. This technique was adopted out to its ease of use relative to a hot-wire. Typical traces are shown in Fig. 11. In this figure, the fluctuations in the signal external to the boundary layer are due to the ambient noise and turbulence in the freestream and are not related to any induced audio signal. It is clear from part (a) of this figure that the differences between a laminar and turbulent signal are distinct. The method was checked against a hot-wire for accuracy. Figures 12 and 13 give the transition lines for $\alpha = 3°$ and 6°, respectively. As can be seen, even low spin rate has a significant effect. The azimuthal behavior is in agreement with theory, c.f., Jacobson and Morton;[10] however, both the peak and valley move towards the nose with increasing $\omega R/V_\infty$ -not in agreement with theory. This apparently is due to the fact that the transition Reynolds number is more strongly affected by spin than the minimum critical Reynolds number. This may be due to an increased disturbance amplification rate.

The growth of the boundary layer was also investigated at $x = 20$ cm. Figures 14(a)-14(e) show the effect of spin on the 90% velocity point. The behavior is expected until the apperance of the large regular waves of as-yet-undetermined origin. These waves caused unusual behavior until transition, at which time the behavior was again as expected. A crossplot of these is shown in Fig. 15 where the characteristic azimuthal variation is as predicted by theory.

The boundary-layer growth along the cylinder was also measured for each of four spin rates (0, 1.4 cps ($\omega R/V_\infty = .13$), 2.7 cps ($\omega r/V_\infty = .25$), and 4.5 cps ($\omega R/V_\infty = .41$). The model was set at an angle of attack of 3° and, due to crossflow, the boundary layer was thicker on the leeward side than on the windward side. However, spin caused the boundary layer on the leeward side to displace in the direction of rotation. With increasing spin rate there was also a noticeable increase in the thickness of the boundary layer on the windward side.

At $\theta = 90°$ spin resulted in the boundary layer being drawn towards the model. This was caused by the fact that both the wall velocity and the crossflow velocity components are in the same direction, which reduces the boundary-layer growth rate. At $\theta = 270°$ the wall velocity and the crossflow velocity component are in opposite directions, causing the boundary layer to thicken. However, none of the spin rates tested caused separation.

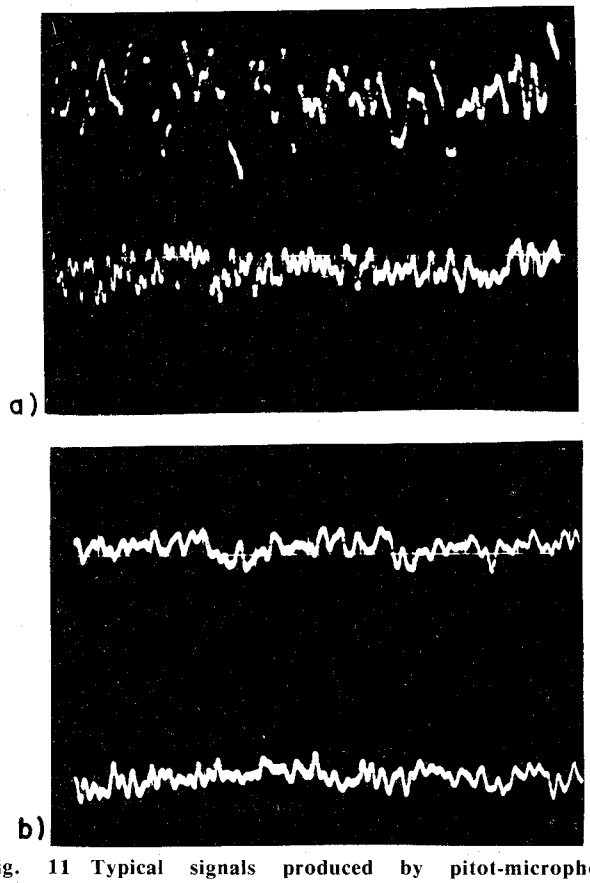

Fig. 11 Typical signals produced by pitot-microphone probe: a) turbulent boundary layer; b) laminar boundary layer. Lower traces are external to boundary layer; upper traces are within boundary layer.

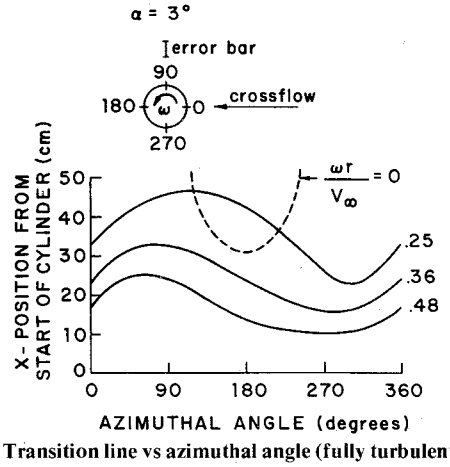

Fig. 12 Transition line vs azimuthal angle (fully turbulent) ($\alpha = 3°$).

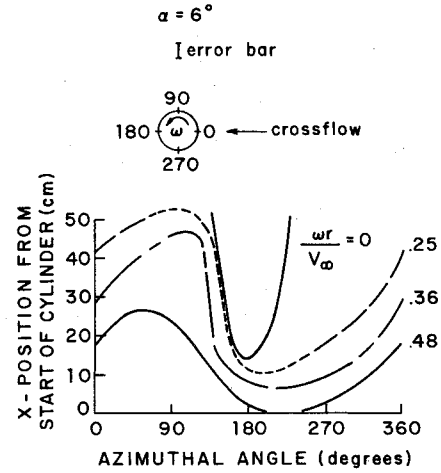

Fig. 13 Transition line vs azimuthal angle (fully turbulent) ($\alpha = 6°$).

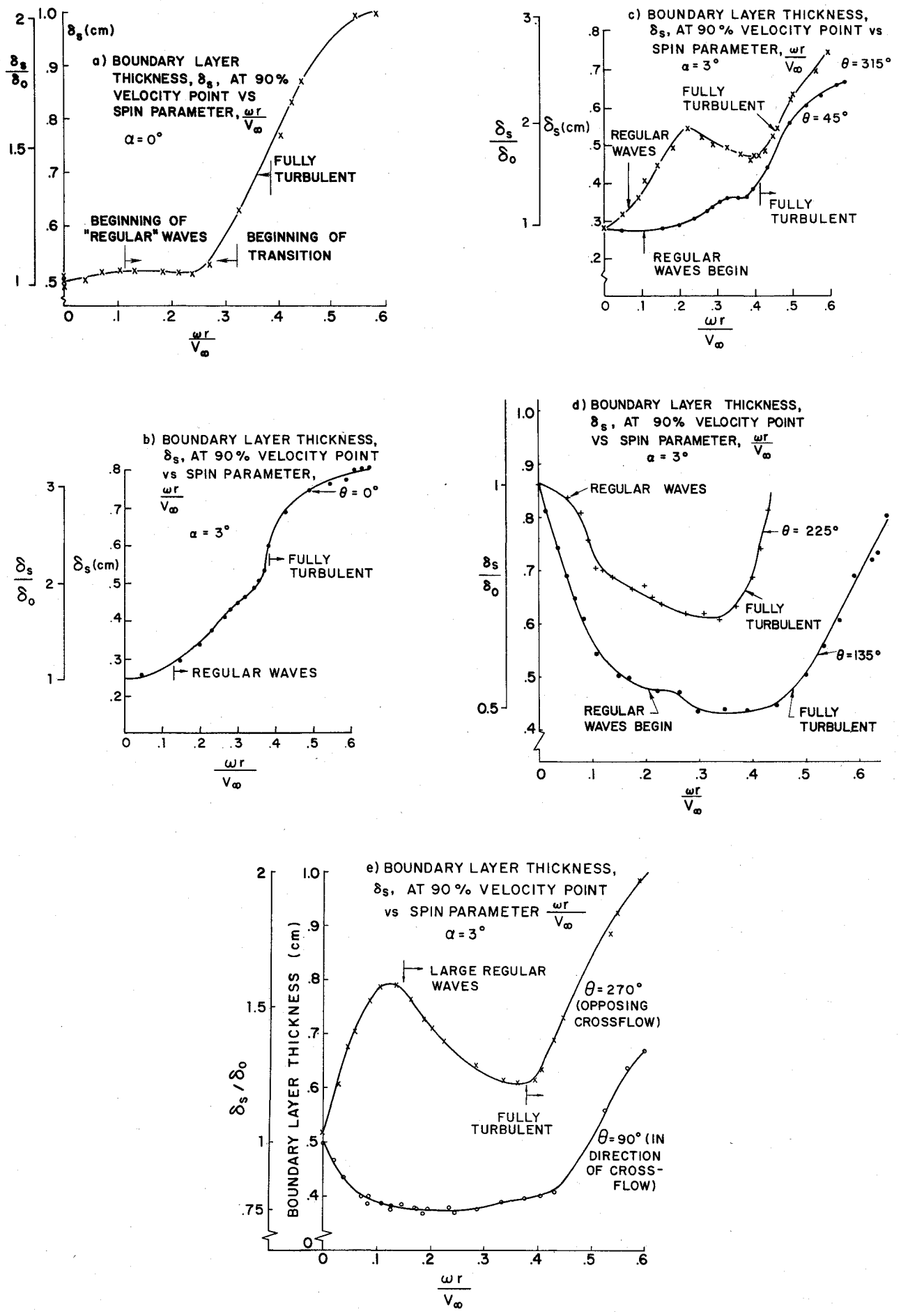

Fig. 14 Effect of spin on boundary-layer thickness: a) $\alpha = 0°$; b)–d) $\alpha = 3°$.

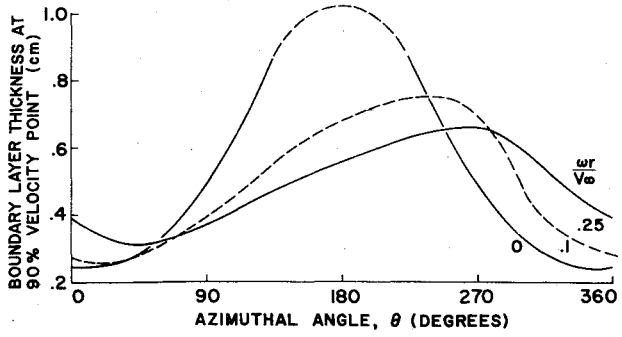

Fig. 15 Boundary-layer thickness at 90% velocity point vs azimuthal angle ($\alpha = 3°$).

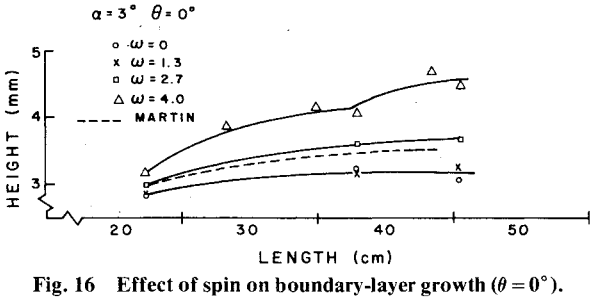

Fig. 16 Effect of spin on boundary-layer growth ($\theta = 0°$).

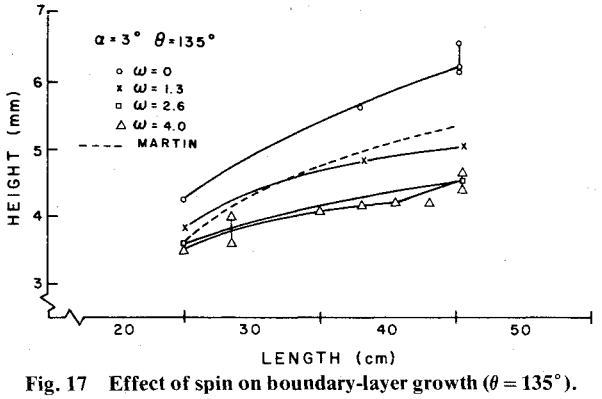

Fig. 17 Effect of spin on boundary-layer growth ($\theta = 135°$).

A comparison was made between the measured boundary-layer growth and that predicted by Martin's formula[7]

$$\delta_x = 1.721 - 1.721\left(\frac{\alpha x}{a}\right)\cos\left(\frac{z}{a}\right) - 1.526\left(\frac{\alpha\omega R}{V_\infty}\right)\left(\frac{x}{a}\right)^2 \sin\left(\frac{z}{a}\right) - \alpha^2\left(\frac{x}{a}\right)^2\left[-.1424 + 1.667\cos 2\left(\frac{z}{a}\right)\right] + .4240\,\alpha^2\left(\frac{\alpha x}{V_\infty}\right)^{1/2} \quad (1)$$

Since δ_x is the displacement thickness, it was necessary to convert it to δ_s.

Martin's formula did not agree very well with the boundary-layer growth predicted from the hot-wire data. This was especially true for the higher spin rates and angles around the body. For instance, as shown in Figs. 16 and 17, at $\theta = 0°$ and 135°, Martin's formula predicts a boundary-layer growth which is relatively equal for all four spin rates, while the hot-wire data shows a distinct difference in the boundary-layer growth for all the spin rates. The effects of spin rate and angle attack are not correctly accounted for Eq. (1), as can be seen in Figs. 18 and 19.

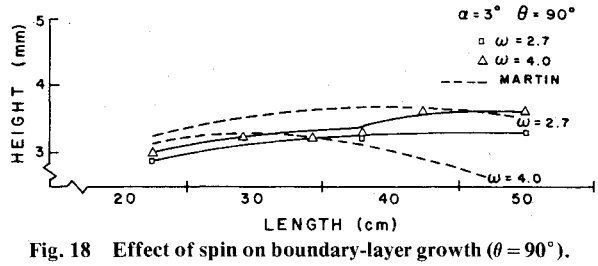

Fig. 18 Effect of spin on boundary-layer growth ($\theta = 90°$).

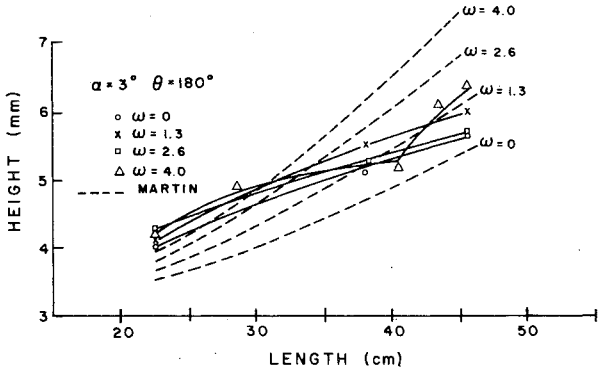

Fig. 19 Effect of spin on boundary-layer growth ($\theta = 180°$).

Conclusions

It has been found that: 1) Spin affects stability and transition of the boundary layer both in reducing the minimum critical Reynolds number and in moving the transition line forward with increasing spin rate. At angle of attack the transition line is also skewed azimuthally due to spin. 2) the boundary-layer thickness and growth rate are modified from flat-plate results due to spin and angle of attack. In the laminar region these results do not agree with Martin's theory. 3) The use of an audio-induced disturbance of known frequency is a viable method for determining the behavior of boundary-layer disturbances.

References

[1] Thorman, H. C., "Boundary Layer Measurements on an Axisymmetric Body with Spin and Yaw," Ph.D. Dissertation, Graduate Aeronautical Labs., California Institute of Technology, Pasadena, Calif. 1958.

[2] Fehrman, A.L., "Effect of Spin and Yaw on Boundary Layer Transition Along a Body of Revolution," A.E. Thesis, California Institute of Technology, 1955.

[3] Furuya, Y., Kakamura, I., and Kawachi, H., "The Experiment on the Skewed Boundary Layer on a Rotating Body," *Bulletin of JSME*, Vol. 9, No. 36, 1966, pp. 702-710.

[4] Jacobson, I. D., "Influence on Boundary Layer Transition on the Magnus Effect on a Spinning Body of Revolution," Dept. of Aerospace Engineering, Ph.D. Dissertation, University of Virginia, Charlottesville, Va. 1970.

[5] Sturek, W. B., "Boundary Layer Studies on a Spinning Cone," Ballistic Research Lab. Rep. 1649, May 1973, Aberdeen Proving Ground, Md.

[6] Sturek, W. B., "Boundary Layer Studies on a Tangent-Ogive-Cylinder Model," Ballistic Research Lab. Rep. 1801, 1975, Aberdeen Proving Ground, Md.

[7] Martin, J. C., "On Magnus Effects Caused by the Boundary Layer Displacement Thickness on Bodies of Revolution at Small Angles of Attack," Ballistic Research Lab. Rep. 870-revised, 1955, Aberdeen Proving Ground, Md.

[8] Barry, M. D. J. and Ross, M. A. S., "The Flat Plate Boundary Layer, Part 2. The Effect of Increasing Thickness on Stability," *Journal of Fluid Mechanics*, Vol. 43, Pt. 4, Oct. 1970, pp. 813-818.

[9] Jacobson, I. D., "Magnus Characeristics of Arbitrary Rotating Bodies," AGARDograph No. 171, Nov. 1973.

[10] Jacobson, I. D. and Morton, J. B., "Influence of Boundary Layer Stability on the Magnus Effect," *AIAA Journal*, Vol. 11, Jan. 1973, pp. 8-9.